

# Spontaneous eye movements in goldfish: oculomotor integrator performance, plasticity, and dependence on visual feedback

B.D. Mensh<sup>a,b,c,\*</sup>, E. Aksay<sup>d</sup>, D.D. Lee<sup>e</sup>, H.S. Seung<sup>a,f</sup>, D.W. Tank<sup>d</sup>

<sup>a</sup> Department of Brain and Cognitive Sciences, Massachusetts Institute of Technology, Cambridge, MA 02139, USA

<sup>b</sup> Department of Biological Psychiatry, Columbia University College of Physicians and Surgeons, New York, NY 10032, USA

<sup>c</sup> Department of Physical Medicine and Rehabilitation, Spaulding Rehabilitation Hospital, Harvard Medical School, Boston, MA 02114, USA

<sup>d</sup> Departments of Molecular Biology and Physics, Princeton University, Princeton, NJ 08544, USA

<sup>e</sup> Department of Electrical Engineering, University of Pennsylvania, Philadelphia, PA 19104, USA

<sup>f</sup> Howard Hughes Medical Institute, Massachusetts Institute of Technology, Cambridge, MA 02139, USA

Received 4 June 2003; received in revised form 11 August 2003

## Abstract

To quantify performance of the goldfish oculomotor neural integrator and determine its dependence on visual feedback, we measured the relationship between eye drift-velocity and position during spontaneous gaze fixations in the light and in the dark. In the light, drift-velocities were typically less than 1 deg/s, similar to those observed in humans. During brief periods in darkness, drift-velocities were only slightly larger, but showed greater variance. One hour in darkness degraded fixation-holding performance. These findings suggest that while visual feedback is not essential for online fixation stability, it may be used to tune the mechanism of persistent neural activity in the oculomotor integrator.

© 2003 Elsevier Ltd. All rights reserved.

**Keywords:** Fixation; Gaze; Saccade; Vergence; Binocular

## 1. Introduction

Goldfish exhibit a spontaneous scanning pattern of horizontal eye movements consisting of saccades and intersaccadic fixations. These fixations are mediated by the oculomotor neural integrator for horizontal eye movements, which converts transient eye-velocity-encoding inputs into persistent eye-position-encoding outputs. Due to the tractability of applying invasive techniques such as intracellular recording, optical imaging, and reversible pharmacologic lesions in awake, behaving goldfish (Aksay, Baker, Seung, & Tank, 2000; Graf, Spencer, Baker, & Baker, 1997; Pastor, Cruz, & Baker, 1994), this species has emerged as an important model system for the study of integrator physiology. Surprisingly, however, there have been no extensive quantitative characterizations of spontaneous eye

movements in goldfish using modern, high-resolution measurement techniques. The present study provides this foundation and in doing so, addresses several hypotheses pertaining to oculomotor control.

Imperfections in oculomotor integrator performance result in drift of the eyes during fixations. Visual feedback has the potential to correct these imperfections by providing the integrator with a retinal-slip-based error signal. A distinction can be made between an “online” role of this feedback to stabilize fixations as they are occurring in real time and a “tuning” role (also called “parametric feedback”), in which the feedback induces plasticity in cellular properties of the integrator in order to improve its performance during future fixations (as in the models of Arnold & Robinson, 1992).

An online role for visual feedback has been suggested in humans by noting immediate increases in fixation drift-velocity with the onset of darkness (Becker & Klein, 1973; Hess, Reisine, & Dursteler, 1985; Skavenski & Steinman, 1970). A similar finding has also been reported in goldfish (Hermann & Constantine, 1971), although in this study the animals were spinalized and the recording techniques were different between the light

\* Corresponding author. Address: Department of Brain and Cognitive Sciences, Massachusetts Institute of Technology, Cambridge, MA 02139, USA. Tel.: +1-617-452-4976; fax: +1-617-452-2913.

E-mail address: [vision@mensh.com](mailto:vision@mensh.com) (B.D. Mensh).

and dark conditions. It is important to note that in addition to providing spatial contrast cues for retinal-slip computations, the presence of light may also induce a tonic input from the retina to the central nervous system which may have effects on neuronal recruitment.

Evidence for an integrator-tuning role of visual feedback in humans comes from patients with acquired blindness, who exhibit fixation drift-velocities much larger than those observed in normal subjects in the dark (Kompf & Piper, 1987; Leigh & Zee, 1980). No evidence of a tuning role for visual feedback has been reported in the goldfish.

We investigated the role of visual feedback in oculomotor integrator performance in the unanesthetized goldfish by measuring spontaneous fixation drift-velocity as a function of eye position in the light and during brief and extended periods of darkness. This position-velocity relationship (the “ $P-V$ ” plot of Becker & Klein (1973), also see the discussion in Goldman et al. (2002)) is of particular interest because of its implications for reverberating circuit models of the integrator. By comparing  $P-V$  plots measured here in the goldfish with those in the human, we can assess the appropriateness of studying the goldfish in order to understand vertebrate oculomotor neural integrator principles in general. This comparison is also interesting considering the size disparity between the goldfish integrator, which has 30–50 neurons unilaterally (Pastor et al., 1994), and that in the primate, where the comparable number is in the thousands (medial vestibular nuclei and prepositus hypoglossi, Cannon & Robinson, 1987).

The present study uses the scleral search-coil method to acquire eye-position data at a spatial resolution of several arc-minutes and a temporal resolution of milliseconds. In addition to addressing the specific hypotheses outlined above, we analyzed these data with respect to saccade metrics, vergence control, binocular coordination, nasal-temporal symmetry, vertical gaze, range of motion, and stretch movements in order to generate the most comprehensive and accurately quantified characterization of spontaneous eye movements in awake, restrained goldfish to date. This complements the long history of the goldfish as a model organism in vision research (e.g., Aksay et al., 2000; Easter, 1975; Johnstone & Mark, 1969; Neumeier, 1984; Pastor, Torres, Delgado-Garcia, & Baker, 1991) and serves as a foundation for ongoing studies of oculomotor control.

## 2. Methods

### 2.1. Animal preparation

Twenty-four adult goldfish (*Carassius auratus*, Hunting Creek Fisheries, 30–50 g) were used in this study. Following anesthetization by immersion in water

containing tricaine methanesulfonate (MS222, 1:3000), each goldfish was wrapped in wet gauze and held in air between clamped sponges. The skull above the optic tecta was exposed and covered with a thin layer of cyanoacrylate (Crazy Glue™) to promote adhesion. Four small screws (mx-000-120-fb, Small Parts Inc.), spaced so that the flat head of an 8–32 brass headbolt fit snugly between them, were anchored into the bone. After mechanical positioning, the headbolt was cemented to the screws and skull with dental acrylic. Headbolting required approximately 10 min and was immediately followed by immersion of fish in a recovery aquarium. Within 30 min each subject swam normally. After at least 3 h of additional recovery, the awake subject was transferred to a circular acrylic tank (25 cm diameter) which was filled with room-temperature distilled water. The head was immobilized by attaching the headbolt to a support column held in a fixed position over the tank. The body was immobilized by clamping contoured sponges to its sides, behind the gills. All mechanical support structures were constructed from acrylic, nylon, or ceramic to minimize magnetic field inhomogeneity. In order to minimize gilling movements (which can cause eye-movement artifact(s)), the fish was respired by flowing recirculated aerated water over the gills through a tube which was tapered to fit the mouth.

### 2.2. Eye-position measurement

Eye position was measured using a modification (Aksay et al., 2000) of the scleral search-coil technique (Robinson, 1963). A coil (5.4-mm, 40-turn, Sokymat SA) was sutured to each eye, concentrically surrounding the 3–4 mm pupil, thus leaving the center of view unobscured. The coil leads were loose, allowing the eye to move freely without tension. The experimental tank was mounted inside a Helmholtz coil system (15-in. diameter, CNC-Seattle) which generates the following two perpendicular oscillating magnetic fields: a 60-kHz field parallel to the long horizontal axis of the goldfish and a 90-kHz field parallel to the vertical axis. After pre-amplification, the signal from each of the two eye coils was separated into the vertical and horizontal components by phase-sensitive detectors (CNC). Output voltages were digitized at 200 Hz using a 12-bit A/D converter and custom software.

To calibrate the measurement system before each experiment, the two search coils were mounted on a 3-D protractor which was then placed in the tank so that the coils were in the same location as the eyes of the fish. The offsets and gains on the phase detectors were adjusted to achieve an output of zero volts at zero degrees (defined as the plane in which both coils are parallel to the plane of the two magnetic fields) and 6 V at 30° of purely vertical or purely horizontal rotation. Then for each of nine horizontal rotational positions ( $\theta = -40^\circ$

to  $+40^\circ$  in  $10^\circ$  steps—this was the primary axis of rotation), the protractor was rotated vertically in seven steps ( $\Phi = -30^\circ$  to  $+30^\circ$  in  $10^\circ$  steps—this was the secondary axis of rotation). At each of these 63 positions, the output voltages of the two channels of each phase detector were measured. Under ideal conditions, the expected horizontal ( $H$ ) and vertical ( $V$ ) voltages, as a function of horizontal and vertical angles ( $\Theta$  and  $\Phi$ ) and gains ( $G_h$  and  $G_v$ ) are:

$$\begin{aligned} H &= G_h \sin(\Theta) \cos(\Phi) \\ V &= G_v \sin(\Phi) \end{aligned} \quad (1)$$

These equations were amended as follows:

$$\begin{aligned} H &= G_h \sin(\Theta - \Theta_0) \cos(\Phi - \Phi_0) + H_{\text{off}} \\ V &= G_v \sin(\Phi - \Phi_0) + V_{\text{off}} \end{aligned} \quad (2)$$

where  $\Phi_0$  and  $\Theta_0$  are angle offsets included to account for slight inaccuracy in mounting the coils onto the protractor, and  $H_{\text{off}}$  and  $V_{\text{off}}$  are included to compensate for the non-zero voltage offsets which result from stray loops in the coils. The six calibration parameters ( $G_h$ ,  $\Theta_0$ ,  $H_{\text{off}}$ ,  $G_v$ ,  $\Phi_0$ ,  $V_{\text{off}}$ ) were determined by numerical optimization (Matlab), in a least-squares sense, as the fit between the 63 pairs of measured voltages and the 63 pairs of idealized voltages computed from the above equations. After this calibration procedure, the coils were removed from the protractor and subsequently sutured to the eyes of the goldfish as described above.

Plotted in Fig. 1A are the voltages (open circles) measured during a calibration run and the idealized voltages (gridlines) obtained from the equations above, using parameters that were computed from the calibration as described. The lack of systematic error reveals the well-behaved geometry of the fields and eye coils. The average error of  $0.1^\circ$  is accountable to (a) the electrical noise in the system, which is 10–20 mV ( $0.05^\circ$ – $0.1^\circ$ ), (b) the resolution of the A/D converter, which is 5 mV ( $0.025^\circ$ ), and (c) the inaccuracy of manually positioning the protractor at each of the 63 calibration points, which, based on test–retest measures, was approximately  $0.08^\circ$ . The effective error from random manual-positioning inaccuracies is reduced significantly by averaging over 63 positions, which is an intrinsic feature of the mathematical technique described above. Thus, the sensitivity and full-scale accuracy of the system is between  $0.05$  and  $0.1^\circ$ .

After conversion of the eye-movement data from voltages to angles, the angles were treated mathematically as points on the surface of a globe and then rotated to discount the mounting angle of each individual fish relative to its primary (horizontal) axis of eye motion. The appropriate rotation matrix, parameterized by three Euler angles, was determined from the eye-position data during the initial light condition, excluding “stretch” movements (see below). Two of the Euler angles were

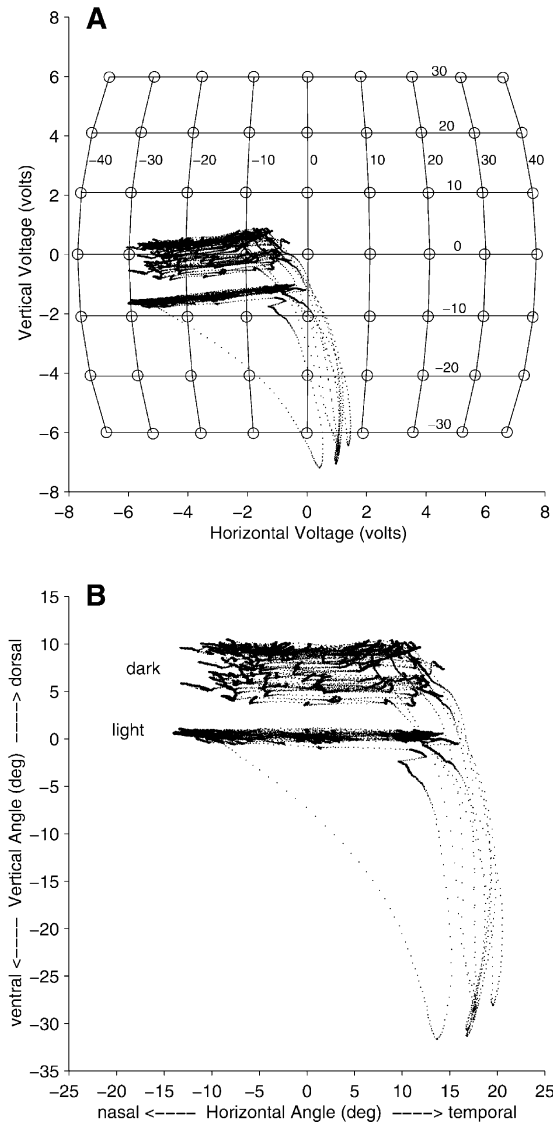


Fig. 1. Calibration. (A) The voltages measured during a protractor calibration run (open circles) and the idealized voltages based on the parameters computed from the calibration equations (gridlines,  $10^\circ$  increments indicated by numerals) are plotted along with the voltages that were measured from the right eye of one goldfish during 10 min of spontaneous eye movements in the light and 10 min in the dark (dots, 5 ms apart). (B) The same data as in A has been converted from volts to degrees, as described in the text.

calculated by minimizing the angular distance of the eyes to the horizontal equatorial plane. The third Euler angle was computed by defining zero azimuthal angle, as follows. In frontal-eyed, foveate animals, this angle is conveniently defined by straight-ahead gaze. Because the goldfish is lateral-eyed, we defined zero azimuthal angle in each eye empirically as the mean of the 5th and 95th percentile of all horizontal angles in the data set for each goldfish described above. An example of the calibration and rotation is shown from Fig. 1A (voltages) to Fig. 1B (rotated angles).

### 2.3. Stimulus conditions

For all 24 subjects, no optokinetic or vestibular stimuli were applied. There were two conditions: light and dark. In the light condition, ambient fluorescent room lights were on. The subject's visual environment consisted of objects in the laboratory and the contents of the transparent experimental tank, which ranged in distance (from the eyes) from 10 cm to 2 m. Surrounding the experimental tank with a high-contrast grating had no effect on drift-velocities or saccade pattern (data not shown). In the dark condition, stray light in the darkened room was prevented from reaching the experimental setup by covering it with three layers of optical black cloth. Animal storage, surgery and experiments were conducted at room temperature. Due to the absence of thermostat-control, temperature variations of up to 2 °C were possible.

In 20 goldfish, spontaneous eye positions were monitored for 10 min in the light, then 10 min in the dark. In the other four goldfish, the protocol was lengthened in order to assess longer-term stationarity and plasticity. This protocol consisted of one hour in the light, one hour in the dark, then another hour in the light. For each subject, Euler angles were always computed on the initial lights-on data and then applied to all the data from that subject.

### 2.4. Analytic methods

Saccades were identified by thresholding the eye velocity at 5 deg/s. A fixation was defined as the portion of the intersaccadic interval beginning 500 ms after the previous saccade (to allow decay of viscoelastic orbital mechanics) and ending 100 ms before the subsequent saccade. Each fixation of at least 1 s in duration was fit by linear regression, from which an average eye position and drift-velocity were obtained (see Fig. 2B). The choice of linear regression was made after preliminary analyses revealed negligible difference between exponential fits and linear fits, presumably because fixations were much briefer than the time constant of the oculomotor integrator. In cases where mild exponential components do exist, linear regression provides an average of the slowly changing eye velocity over the course of a fixation.

To determine the quality of the linear-regression fit for each fixation, the sum-squared error was computed. For each experimental period, the 10% of fixations which had the highest sum-squared error were discarded. The principal causes of high sum-squared error were spontaneous gilling movements (which are mechanically transmitted to the eyes) and very small saccades that were missed by the velocity-thresholding algorithm. Fixations immediately before and after stretch movements were also discarded. Using this

protocol, approximately 40% of fixations qualified for inclusion into drift-velocity-versus-position-plots. Most exclusions were due to fixations being briefer than our criterion of 1 s.

## 3. Results

### 3.1. Basic characteristics of spontaneous eye movements

Fig. 1B displays all of the eye positions observed in one goldfish eye in the light and in the dark. Horizontal range of motion (ROM) was quantified by subtracting the position of the most nasal fixation from the position of the most temporal fixation. In the light, the horizontal ROM for this subject was 28.1° (median for all eyes was 29.2°; range was 16.2–35.8; there was a strong correlation between the ROMs of the left and right eyes of each fish,  $r = 0.92$ ) and the vertical ROM was about 2° (similar for all eyes).

When the lights were turned off, there was an immediate 5° dorsal (upward) shift in gaze, which increased to 10° during the 10 min in the dark. A dorsal shift was observed in all eyes and ranged from 4° to 15°. Also in the dark, the horizontal ROM decreased in all cases (median decrease 3.0°; range 0.2–8.3). The main axis of movement in the dark was nearly parallel to that in the light (the angle between the two axes was typically less than 10°). In both conditions, several large ventral/temporal excursions of the eyes are evident. These have previously been referred to as “stretches” and are discussed below. They are excluded from the calculations of range of motion above. In the following, we ignore changes in the vertical component and focus on the horizontal component of eye movements.

In Fig. 2A, a time-domain sequence of eye movements is displayed. Grossly, the epoch consists of three types of eye movements: (a) fixations, during which the eyes move relatively slowly, (b) saccades, during which both eyes move rapidly and simultaneously (and usually in the same direction), and (c) a “stretch”, during which both eyes move to extreme temporal positions. The epoch in Fig. 2A begins with both eyes making two rightward saccades to reach the extreme right gaze position, followed by four leftward saccades resulting in both eyes reaching the extreme left gaze position. In both the light and the dark, we typically observed this scanning pattern of saccades, in which both eyes fixate toward one extreme, then span the range of motion in 2–4 saccades to arrive at the other extreme. Fixation duration was typically 1–4 s (median 2.03 s) and was slightly longer in extreme positions of gaze than in middle positions. In the long-term protocol, fixation durations increased by nearly twofold during the hour in the dark. Stretch movements occurred an average of once every 2.3 min in the light and in the dark.

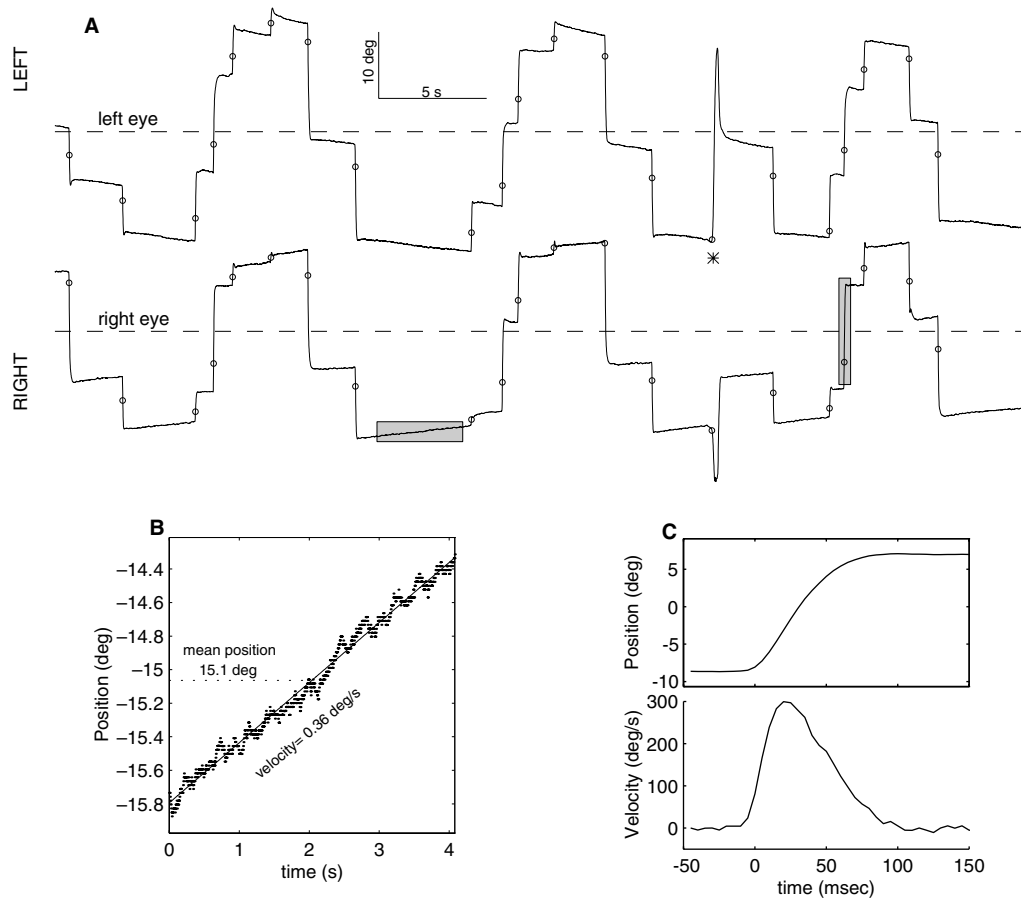


Fig. 2. Spontaneous eye movements. (A) A 45-s epoch of the horizontal component of eye position from both eyes of one goldfish in the light. Dashed lines represent the center (zero) position for each eye. Circles represent points identified by the saccade-finding algorithm. One stretch occurred (asterisk). (B) Example of a gaze fixation. The fixation shaded in A is expanded. The line of best fit and its mean position and velocity are indicated. (C) Example of a saccade. The saccade shaded in A is expanded and its velocity is plotted beneath it. Saccade amplitude was defined as the difference in position 150 ms after the beginning of the saccade and 50 ms before the beginning of the saccade. The beginning of the saccade was defined as the time at which the velocity became greater than 5 deg/s.

An expanded view of a fixation (Fig. 2B) reveals a slow, unidirectional movement. The linear appearance was typical, although, small amounts of curvature in either direction were occasionally observed. The line of best fit was used to characterize each fixation by two numbers: the mean position and the mean drift-velocity.

Fig. 2C shows a detailed view of a saccade during which most of a  $14^\circ$  movement was completed within 70 ms. The velocity profile shows a rapid acceleration phase, a sharp maximum velocity with virtually no plateau, and a somewhat slower deceleration phase.

### 3.2. Drift-velocity versus position

Fig. 3 shows  $P-V$  plots for the first eight fish measured (of 20 total) in the short-term protocol. In the light (Fig. 3, left column), almost all of the drifts were nasally directed). The magnitudes of the drift-velocities were almost exclusively less than 1 deg/s. When the lights were turned off (Fig. 3, right column), the drift-

velocities became much more variable, but the magnitudes remained small (generally less than 1.5 deg/s), which is similar to the drift-velocities observed in humans (Becker et al., 1973; Hess et al., 1985). In many cases, the  $P-V$  relationship was not simply linear.

Data for all 20 fish of the short-term protocol are summarized in Fig. 4. In Fig. 4A, a mean drift speed was computed for each eye/condition by averaging drift speeds across positions. In order to insure that fixations from each part of the eye-position range contributed equally to the overall mean (and thus neutralize the potential contamination from unequal sampling of eye positions), the data were binned based on eye position prior to averaging (see Fig. 4). For most eyes (26 out of 40), the mean drift speed was somewhat greater in the dark than in the light (median dark/light speed ratio = 1.26,  $p < 0.05$ ).

Fig. 4B shows the average standard deviation of drift-velocity for each eye, also averaged across position bins. The increased drift-velocity variability in the dark

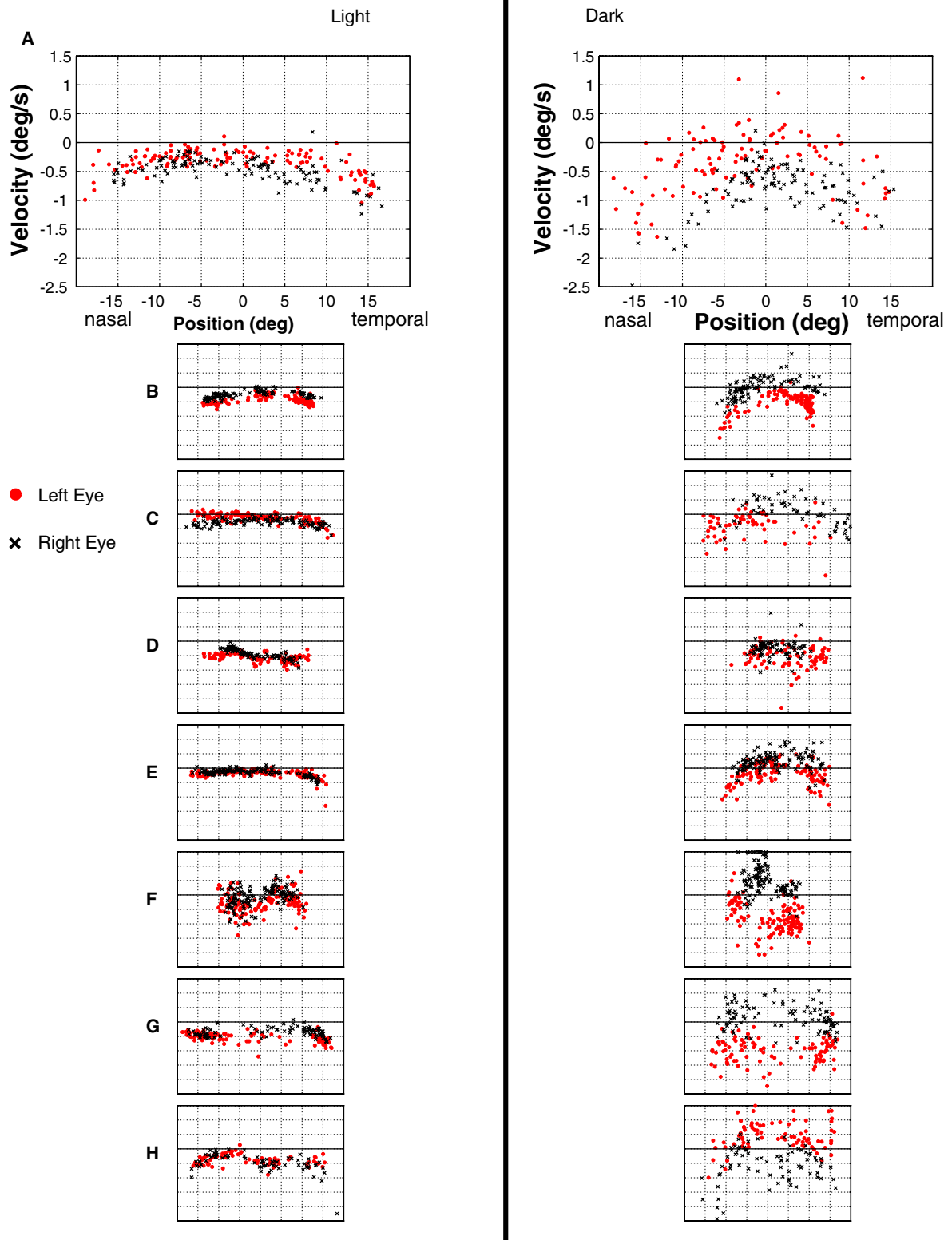


Fig. 3. Gaze-fixation drift-velocity versus position for the 10-min light/10-min dark protocol. Left column is in the light; right column is in the dark. Each of A–H represents data from one of the first eight fish (out of 20 total) tested in this protocol. All plots have identical domains and ranges. For the position axis, nasal (closer to the nose) is negative, temporal is positive. For the velocity axis, nasal (moving towards the nose) is negative, temporal is positive.

condition evident in Fig. 3 is true for all 40 eyes, as all the points lie above the diagonal line of interocular equality.

The correlation in overall drift-velocity variability between left and right eyes of a given fish can also be seen.

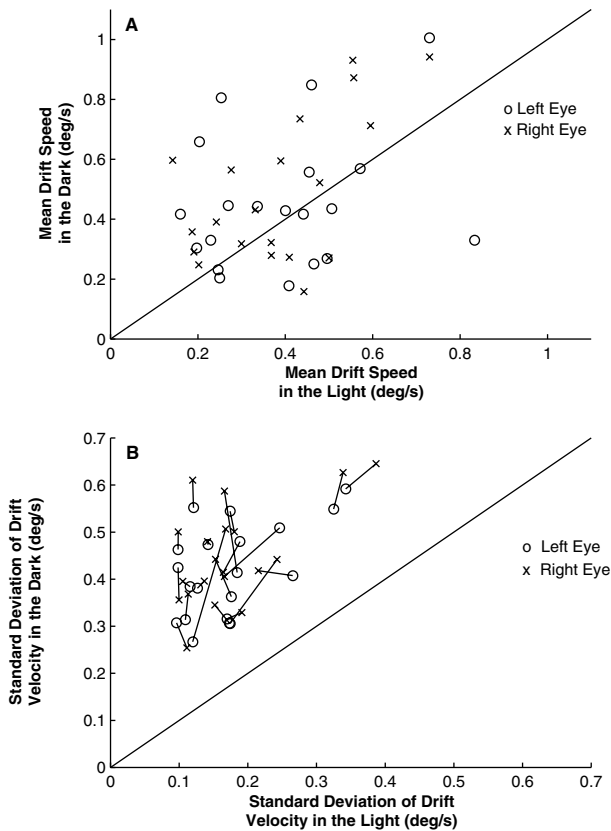


Fig. 4. Summary of group results (20 subjects) for drift-velocity-versus-position data. Fixations were binned by position (5 deg/bin). For each bin, the mean and standard deviation of the drift-velocities were computed. (A) Mean drift speed was computed for each eye and condition (light or dark) by taking the mean of the absolute values of the mean drift-velocities across bins. (B) Standard deviation for each eye and condition (light or dark) was computed by averaging the standard deviations across bins. Data from the left and right eyes of a given fish are linked by a solid line. In both plots, all 40 eyes are shown, light versus dark. The lines of light–dark equality are plotted.

### 3.3. Drift-velocity variability

To further investigate drift-velocity variability, the data were analyzed on a fixation-by-fixation basis. The drift-velocity of each fixation was converted into a Z-score, which indicated how many standard deviations above or below the mean drift-velocity it was relative to other fixations from the same eye, condition, and position (see Fig. 5). This Z-score approximates the residual drift-velocity value which would remain after subtracting a curve of best fit from the drift-velocity-versus-position plots of Fig. 3. Fig. 5A shows the correlation between these residuals in the left and right eyes from a single fish in the dark. That is, when the right eye was drifting to the right more than usual for its position, the left eye was simultaneously drifting to the right more than usual for its position. This was true for most fish in both conditions, as shown in Fig. 5B where 18 out of 20 of the points lie in the upper-right quadrant, indicating a

positive correlation between left and right eye drift-velocity residuals in the light and the dark. In addition, the points are above the line of light–dark equality, indicating that the correlation was stronger in the dark.

The temporal dynamics of drift-velocity residuals were assessed with a modified version of the autocorrelation method, an example of which is illustrated in Fig. 5C. The broad central peak reveals that the residuals were not random on a fixation-by-fixation basis. Rather, they were slowly changing: in this case the drift-velocity residual of a given fixation was positively correlated with those measured up to >10 fixations later. The group data is shown in Fig. 5D, where the median autocorrelation coefficient across the 40 eyes is plotted separately for the light and dark conditions. In the dark, the autocorrelogram was positive in most eyes out to a fixation lag of >40 fixations, which corresponds to 6–8 cycles of the left–right scanning pattern depicted in Fig. 2. No such trend was seen in the light.

### 3.4. Prolonged recordings

The  $P$ – $V$  plots for the subjects in the long-term protocol are shown in Fig. 6. To aid in the analysis, we fit a straight line to each velocity–position dataset. The inverse slope of this line would represent the integrator time constant of a linear system, while the velocity at the center of gaze ( $0^\circ$ ) represents the velocity bias. The relationship between velocity and position was stable throughout the initial hour of lights-on conditions with similar characteristics to the curves in the short-term protocol (Fig. 3). Also as expected from the results of the short-term protocol, when the lights were turned off, the velocities became more variable and most eyes showed decreases in time constant during the first 10 min of darkness. This latter trend did not quite reach statistical significance in the group data of the long-term protocol ( $p = 0.06$ , Wilcoxon signed rank test), presumably because the  $n$  was smaller than in the short-term protocol. During the hour in the dark there was a degradation of fixation performance in all eyes: the slope (negative) increased in absolute value ( $p < 0.01$ ) from  $0.038 \pm 0.021$  (mean  $\pm$  standard deviation)  $s^{-1}$ , corresponding to a slightly leaky integrator with an average time constant of 26 s, to  $0.084 \pm 0.048$   $s^{-1}$ , corresponding to a more leaky integrator with a reduced average time constant of 12 s.

During the first 10 min after the lights were turned back on, the slope of the  $P$ – $V$  plots did not change systematically compared to the end of the dark condition. During the ensuing hour, however, the  $P$ – $V$  plots approached their pre-dark form as evidenced by decrease in the absolute value of the slope ( $p < 0.01$ ) from  $0.074 \pm 0.040$   $s^{-1}$  at the beginning to  $0.027 \pm 0.021$   $s^{-1}$  at the end.

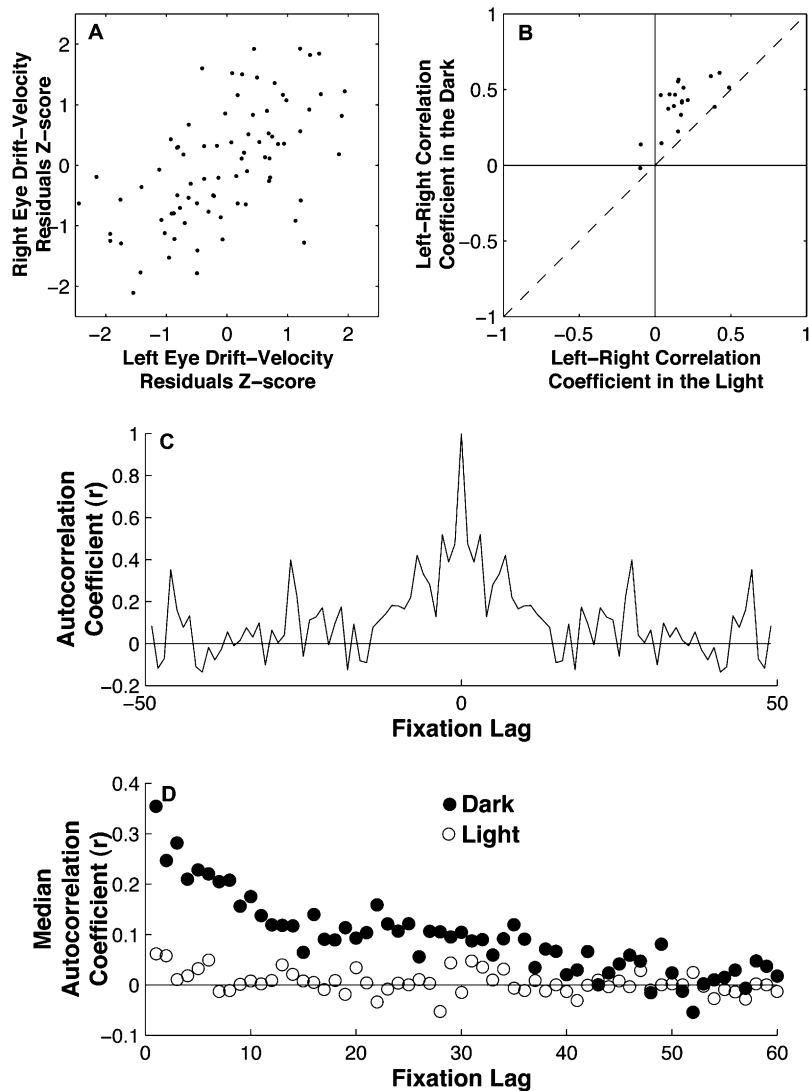


Fig. 5. Drift-velocity residuals. The drift-velocity of each fixation for a given eye/condition was Z-transformed by grouping it with all other fixations within  $3^\circ$  of eye position and then computing a drift-velocity Z-score for that fixation equal to the number of standard deviations above (+) or below (-) the group mean drift-velocity. Leftward positions and velocities are defined as positive for both eyes. (A) Left eye versus right eye Z-score residuals are shown for fish #5 in the dark ( $r = 0.51$ ,  $p < 0.001$ ). Each point represents data from both eyes during one fixation. (B) Correlation coefficients between drift-velocities of left and right eyes for each condition. All 20 subjects of the 10-min protocol are plotted. (C) Autocorrelogram of drift-velocity residuals for fish #12, right eye, dark condition. Fixations were ordered sequentially in time for the 10-min epoch and autocorrelation was computed on the residual Z-scores. The value at a fixation lag of 10, for example, indicates the correlation coefficient ( $r$ ) between all pairs of fixations that were 10 fixations apart in time. (D) Group data for autocorrelations. For each fixation lag, the median  $r$  across all 40 eyes is shown separately for dark and light conditions. Significance values were computed for each eye and fixation lag. In the dark, for a fixation lag of 1, 26 out of 40 eyes had a correlation significance of  $p < 0.05$ . For a fixation lag of 5, 17/40 were significant; for a lag of 10, 11/40 were significant; at a lag of 20, 8/40 were significant; at a lag of 30, 7/40 were significant.

### 3.5. Vergence

Because the goldfish is lateral-eyed, the visual axes of its two eyes always diverge from each other. In order to analyze interocular coordination in the goldfish, we operationally defined convergent eye movements as those which decrease the angle between the two visual axes, divergent movements as those which increase it, and non-vergent movements as those which do not change it (see Fig. 7 legend). In this sense, we are using

the term “vergence” to mean “angle between the two visual axes.” It is important to note that for frontal-eyed, foveated animals, these terms have specific associations with stereopsis and accommodation which do not apply to the lateral-eyed, avoate goldfish. We are simply using these terms to describe the coordination between movements of the two eyes.

The coordination between the left and right eyes, evident in Fig. 2A, is depicted more fully in the vergence-plane plot of Fig. 7A. Although this plot of data

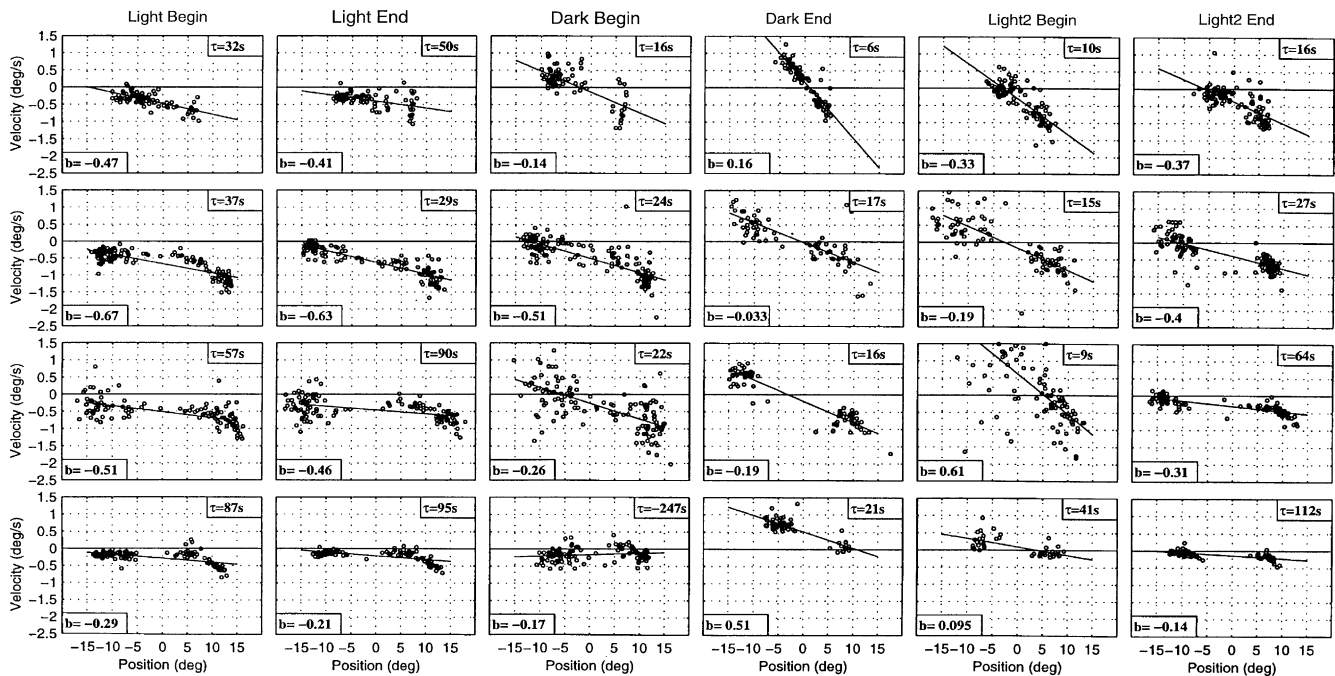


Fig. 6. Fixation drift-velocity versus position for the one-hour light/one-hour dark/one-hour light protocol. Each row is data from the left eye of one of the four fish in this protocol. Columns labeled “Begin” comprise data from the first ten minutes of each hour; those labeled “End” are from the final ten minutes. All plots have identical domains and ranges, the same as in Fig. 3. In the upper-right corner of each plot is the estimated time constant determined from the slope of the dashed line through the data determined by a least-squares fit. The velocity bias, determined from the velocity at  $0^\circ$  of the best fit line, is shown in the lower left corner of each plot.

from a single goldfish reveals a clear correlation between the two eye positions, there is a significant amount of variability in vergence across the range of visual angles. That is, for a given left eye position, the right eye position varies over a range of  $5^\circ$ – $10^\circ$ , and vice versa. This degree of correlation was observed in all fish.

For the particular goldfish depicted in Fig. 7A, the eyes are  $5^\circ$ – $10^\circ$  more convergent in the middle third of their range of motion than they are at their extremes, as indicated by the curvature in the cloud of data. For the same fish in the dark (Fig. 7B), the curvature is less pronounced and the eyes are overall more divergent than in the light. Looking at the vergence-plane plots from all subjects, these patterns were not consistent: some of the subjects had very little curvature in their data clouds; some had double curvature; some were tilted relative to the iso-vergence (diagonal) line.

To determine if stretches play a role in recentering or vergence-resetting, eye positions before and after stretches were analyzed. Eye positions before stretches were distributed randomly in the vergence-plane data cloud for all subjects. In 80% of goldfish (one example shown in Fig. 7A and B), the first fixation after each stretch was in a highly divergent region of the vergence plane (circles). The subsequent saccade typically brought the eyes back into the data cloud (i.e., the highly divergent stretch is matched by a subsequent, highly convergent saccade). In the other 20% of subjects, the first post-

stretch fixations were in the main cloud of data, roughly in the center of the range of motion for each eye.

Finally, the vergence of saccades was analyzed. Fig. 7C and D show data pooled from the first 12 subjects. In both light (Fig. 7C) and dark (Fig. 7D), small saccades tended to be divergent and large saccades tended to be convergent. When looked at separately, each subject displayed this pattern. In addition, most saccades resulted in a decrease in vergence, in that the vergence *before* saccades was negatively correlated with the vergence *after* saccades (data not shown). This vergence-regulating feature in goldfish saccades has been previously shown by Easter (1971).

To summarize the influences of the different types of eye movements on vergence: (a) drifts during fixations were convergent in the light and convergent or non-vergent in the dark (from Fig. 3); (b) typically-divergent stretch movements combined with their typically-convergent post-stretch saccade were together non-vergent; and (c) small saccades were divergent, large saccades were convergent.

### 3.6. Saccade metrics

The position and velocity profiles of a family of saccades are shown in Fig. 8A and B. For all saccade amplitudes, a rapid acceleration phase is followed by a slower deceleration phase, with little or no velocity

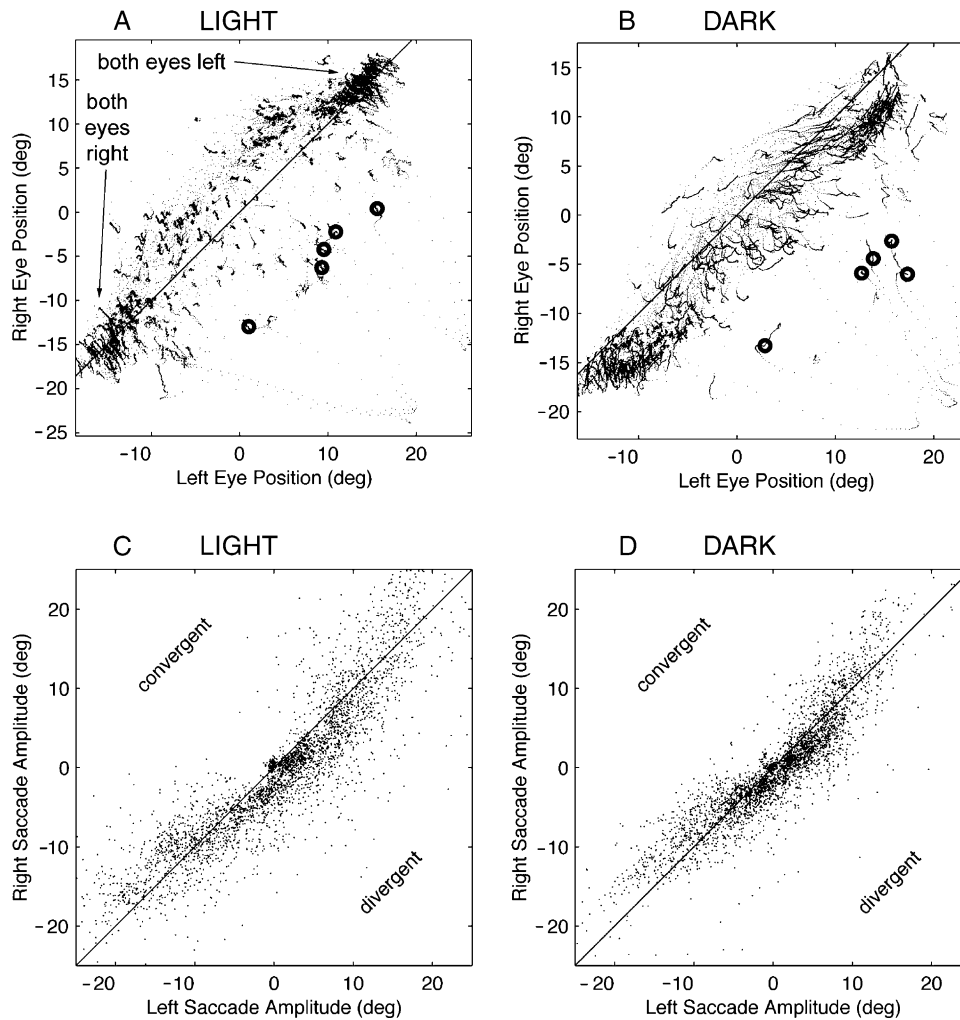


Fig. 7. The vergence plane: right versus left horizontal eye position from one fish for 10 min in the light (A) and 10 min in the dark (B). Leftward positions and velocities are defined as positive for both eyes. Circles represent positions at one second after the peak excursion of a stretch (five stretches occurred in each 10-min period). Diagonal lines represent iso-vergent left–right position-pairs. Zero vergence is defined as the angle between the eye positions when both eyes are in their center of gaze (as defined above in Section 2). Because the zero positions for each eye are necessarily arbitrary in avoate animals such as the goldfish, these lines could be shifted parallel in either direction without affecting the interpretation of the figure. Moving up/left in this plane represents increasing convergence of the eyes (right/down is increasing divergence). For all axes, positive values are leftward gazes and negative values are rightward. Horizontal and vertical axes are scaled equally. Right versus left saccade amplitude for 10 min in the light (C) and 10 min in the dark (D) for the first 12 fish pooled together. Diagonal lines represent zero change in vergence (and thus do not depend on the arbitrary center-of-gaze definition). Points above/left of this line represent convergent saccade pairs, those below/right are divergent. Saccade amplitude is defined in Fig. 2.

plateau between them. Larger saccades have longer durations than smaller saccades. Note that during each of the smallest three saccades, there is a pulse-step mismatch; in this case, the eye slightly overshoots its eventual post-saccadic position. For temporad (temporally directed) saccades, nearly every fish exhibited small ( $<1^\circ$ ) overshoots for small saccades but undershoots of up to  $3^\circ$  for large saccades. Nasad saccades were more variable: most subjects exhibited very little pulse-step mismatch, some had undershoots, some had overshoots.

In Fig. 8C, peak velocity versus amplitude is plotted for both nasad and temporad saccades. The relationship is fairly linear for this subject. In many subjects, the

peak velocity increased sublinearly for large saccade amplitudes ( $>15^\circ$ ). Nasad saccades were slightly faster than temporad saccades, as indicated in Fig. 8D. In addition, saccades were faster in the light than in the dark (see figure for statistics).

The simultaneity of saccades between the left and right eyes, evident in Fig. 2A, was analyzed in detail by taking the absolute time at which each eye reached its half-maximum velocity during a saccade. Subtracting the time of one eye from that of the other yields a measure of interocular timing difference, as displayed in Fig. 8E. Ninety-six percent of the saccade pairs were synchronous to within 5 ms (median = 92% for all fish in

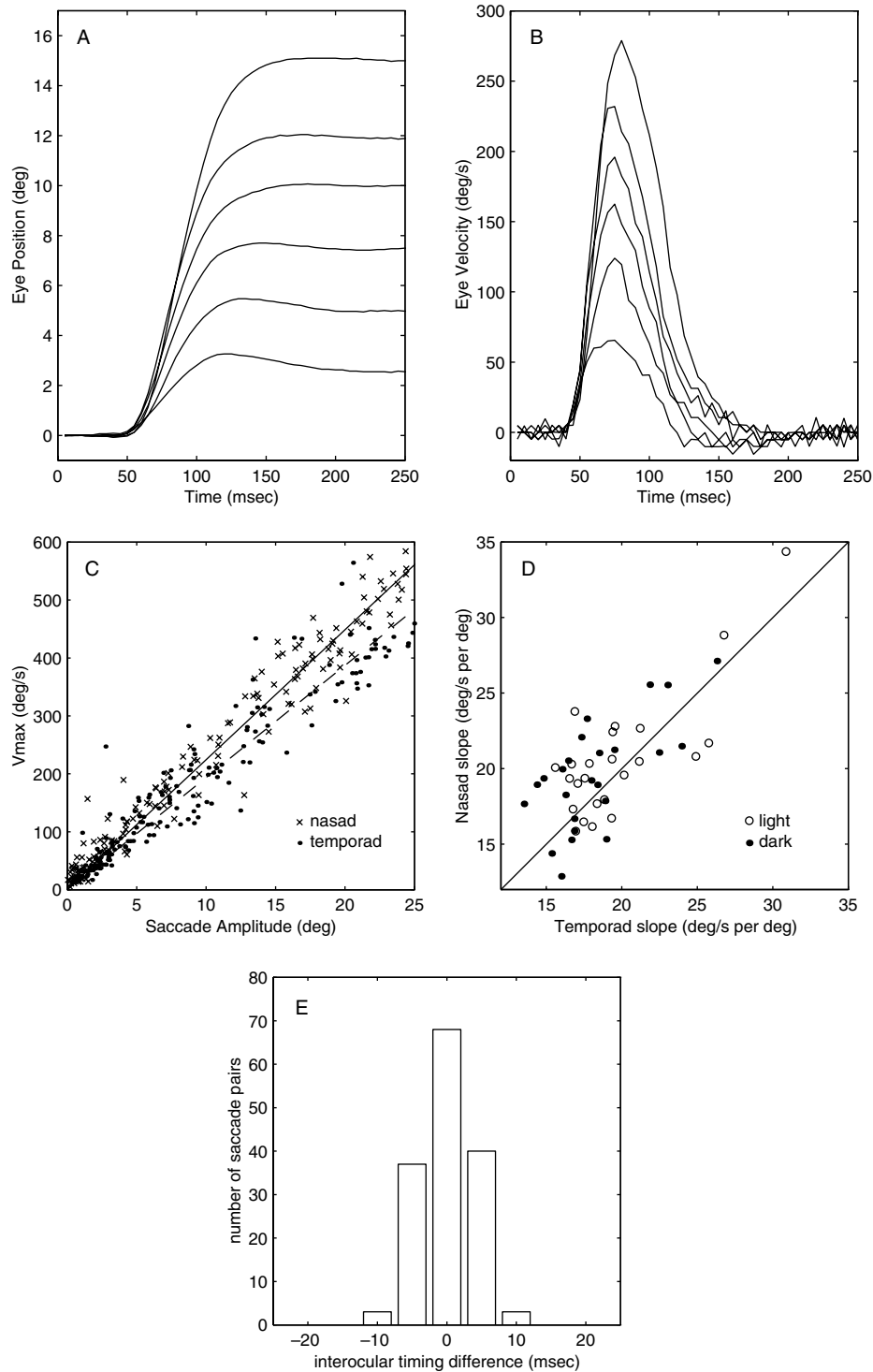


Fig. 8. Family of saccades (A, B): six saccades in the same direction from one goldfish eye. (A) Position versus time: for each saccade, its starting position is subtracted in order to collocate them. In order to synchronize them (for display purposes only), time = 50 ms for each saccade is defined as the time at which its velocity became greater than 5 deg/s. (B) Velocity versus time for the same six saccades. (C) Peak velocity ( $V_{max}$ ) versus saccade amplitude for nasad and temporad saccades. Lines of best fit, constrained to pass through the origin, are drawn (solid—nasad saccades; dashed—temporad saccades). (D) Nasad versus temporad slopes of best fit lines for the first 12 fish in light and dark. Diagonal line is the line of equal slope. Median slopes 19.8 deg/s/deg for nasad, 18.0 deg/s/deg for temporad, 29 out of 48 are larger for nasad ( $p = 0.06$ , sign test). Median slopes 19.4 deg/s/deg for light, 18.4 deg/s/deg for dark, 36 out of 48 are larger for light ( $p < 0.0001$ , sign test). (E) Interocular synchrony histogram. For each saccade pair in which both left and right eyes moved more than  $2^\circ$ , the point in time at which the right eye velocity reached half of its maximum for that saccade was subtracted from the analogous point in time for the left eye. These 151 saccade pairs are from one fish during 10 min in the light.

the light). In the dark, the eyes were slightly less synchronized (median = 82%, sign test  $p = 0.02$  for difference between light and dark). For all subjects, the peak of the histogram was at 0 ms, indicating that no goldfish displayed a systematic lead or lag of one eye.

#### 4. Discussion

##### 4.1. Fixation drift-velocity in goldfish compared to humans

The magnitude of the drift-velocities in the goldfish of the current study was comparable to those observed previously in humans (rarely greater than 1.5 deg/s in the dark or the light, Becker et al., 1973; Hess et al., 1985). This quantitative similarity supports the relevance of studying the goldfish oculomotor integrator in order to understand vertebrate integrators in general. The performance of the goldfish system is particularly impressive considering that its oculomotor integrator has at least an order of magnitude fewer neurons than the analogous structure in humans (Cannon et al., 1987; Pastor et al., 1994).

The finding of comparable integrator performance across disparate network sizes has implications for network models of the integrator, which are generally sensitive to tuning of positive feedback. If the synaptic weights of the model network are perturbed in some way, the performance of the integrator drops, as evidenced by a change in the time constant or bias. Cannon, Robinson, and Shamma (1983) argued that network integrators become more robust to mistuning with increasing size. In light of the current results, this would require that synaptic weights in the goldfish be much more accurately maintained than those in the human, in order to achieve comparable performance. By contrast, Seung (1996) disputed the relationship between network size and mistuning robustness, which is consistent with the current results without requiring finer synaptic control in the goldfish.

##### 4.2. Light versus dark: the role of visual feedback and tuning

For a given eye position, drift-velocity was substantially more variable in the dark than in the light (Fig. 4B). This variability was well correlated between left and right eyes (Fig. 5A and B), indicating that a common velocity-bias signal is being transmitted to oculomotor nuclei bilaterally. Although seemingly random, this signal is slowly changing, as evidenced by its temporal correlations (Fig. 5C and D). Because the typical left-right scanning pattern of saccades comprises 5–6 fixations per cycle (see Fig. 2), this slowly changing bias spans many scanning cycles and is thus not simply

dependent on eye position. The presence of light is apparently able to prevent or compensate for this velocity bias. It is important to note that there are at least two potential mechanisms for the role of light in these experiments: either as a retinal-slip error signal to provide specific information about the drift of the eyes or, more simply, by providing tonic retinal excitation which may impact on cell recruitment downstream in the oculomotor system.

In a previous comparison between light and dark behavior, Hermann and Constantine (1971) “did not observe a post-saccadic slow counter slew” in the light, but did in the dark. This led them to suggest that visual feedback was stabilizing the goldfish’s gaze. Because their measurement systems were different for light and dark conditions, both of which were uncalibrated and had unknown sensitivity, it is likely that the drifts in the light were simply too small to be resolved. The quantitative similarity we observed between drift-velocities in the light (mean = 0.39 deg/s) and in the dark (mean = 0.47 deg/s) in the 10-min protocol supports the notion that visual feedback to the oculomotor integrator plays only a small online role in fixation stability.

While the presence of light does not appear to be essential for integrator function on short time scales, it may be important for maintaining the performance of the integrator over longer time scales. Arnold and Robinson (1991, 1992) postulated that visual feedback could be used as an adaptive mechanism to tune the strength of synaptic connections in the integrator. This hypothesis is supported by our observation of a degradation in fixation stability during one hour in the dark. Ethologically, this “dark de-tuning” presumably occurs in the goldfish each night and is reversed by “light re-tuning” the next day. Indeed we observed consistent improvements in drift-velocity during the post-darkness hour in the light. Further studies will be required to assess the role of the optokinetic response during this retuning phase.

Our observation of nasally directed drift in the light (Fig. 3) is consistent with data from Easter (1971), who reported convergence between the eyes during intersaccadic intervals in the light. He reported total drifts of typically less than 5 degrees per interval, but did not give instantaneous drift-velocities or data from dark conditions.

##### 4.3. Implications of velocity-position relationship for oculomotor integrator models

As can be seen from Figs. 3 and 6, fixation performance, as quantified by the  $P-V$  plot, varies from fish to fish. Similar intersubject variability in normal humans has previously been described (Becker et al., 1973; Hess et al., 1985). Even in a single fish, the relationship varies over time, as shown in Fig. 6. It also depends on lighting

conditions, as evidenced by the light–dark differences in Figs. 3 and 6. Variability in fixation performance over time has also been reported in pathological human subjects, and normal subjects after adaptation with visual-vestibular conflict (Jones, 1977; Tiliket, Shelhamer, Roberts, & Zee, 1994). All of these types of variability have been modeled in terms of parametric changes in a neural integrator (Leigh & Zee, 1991).

According to the integrator model, the dynamics of fixation are governed by the equation

$$\frac{dE}{dt} = -\frac{E}{\tau} + b \quad (3)$$

where  $E$  is eye position,  $dE/dt$  is eye velocity,  $b$  is a bias, and  $\tau$  is the time constant of fixation. For an ideal integrator, the time constant  $\tau$  is infinite, and the bias is zero. In other words, both the slope and intercept of the velocity–position relationship vanish. Between saccades, which are driven by pulse inputs to (3), eye position is constant in time ( $dE/dt = 0$ ). However, real integrators fall short of the ideal. A negative slope makes the integrator *leaky*, a positive slope makes it *unstable*, and a non-zero intercept makes it *unbalanced*. All three of these cases are schematically illustrated in Fig. 9.

The unbalanced integrator of Fig. 9A has unidirectional drift, lacking a *null position*, or eye position at which drift vanishes. A small imbalance of roughly 1 deg/s is often seen in normal human subjects (Becker et al., 1973; Hess et al., 1985). In pathological cases the bias can be much greater. For example, unilateral damage to a vestibular labyrinth unbalances input to the integrator, and the resulting nystagmus has linear slow phases, with velocity roughly independent of eye position.

In the leaky integrator of Fig. 9B, the slope of the velocity–position relationship is negative, and the drift is centripetally directed towards a null position. Since drift-velocity decreases as the eye approaches the null position, eye position decays exponentially during intersaccadic time intervals. If the magnitude of the drift-velocity is small, it may be difficult to distinguish exponential from linear drift, but the exponential behavior is clear if the time constant is short and the imbalance is small. Slight leakiness is commonly seen in normal human subjects, with a time constant of roughly 20s (Becker et al., 1973; Hess et al., 1985). Small increases in leakiness lasting for minutes can be induced through adaptation with visual-vestibular conflict

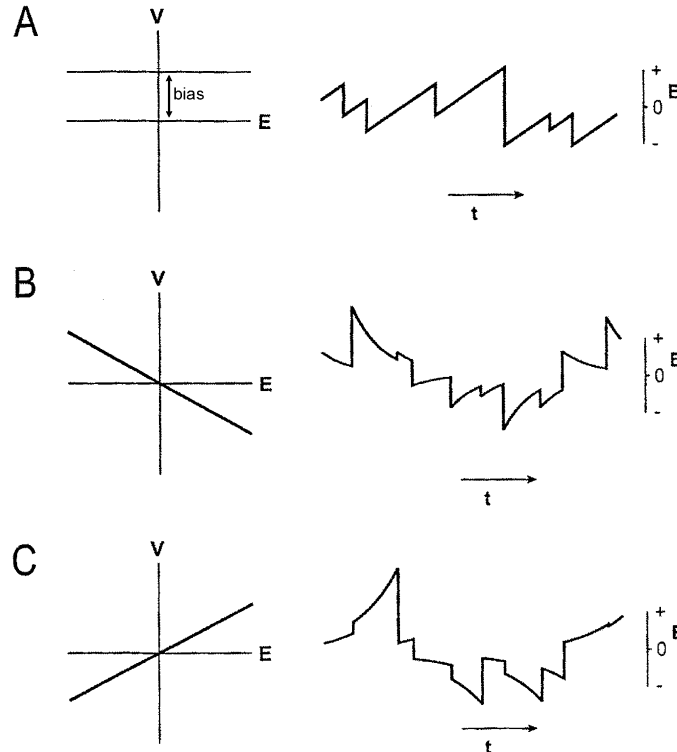


Fig. 9. Linear models of the integrator. If the integrator is perfectly tuned, drift-velocity ( $V$ ) is zero at all eye positions ( $E$ ). If the integrator is imperfectly tuned, the relationship between drift-velocity and eye position is linear. (A) An unbalanced integrator (large intercept and small slope) has unidirectional drift, with no null position. The nystagmus has linear slow phases. (B) A leaky integrator (small intercept and negative slope) has centripetal drift to a null position. The nystagmus has exponentially decaying slow phases. (C) An unstable integrator (small intercept and positive slope) has centrifugal drift away from a null position. The nystagmus has exponentially increasing slow phases.

(Tiliket et al., 1994). Severe leakiness is seen in the clinical disorder of gaze-evoked nystagmus (Leech, Gresty, Hess, & Rudge, 1977), and can also be induced pharmacologically (Corbett, Jacobson, Thompson, Hart, & Albert, 1989; Rottach, Wohlgemuth, Dzaja, Eggert, & Straube, 2002).

The unstable integrator of Fig. 9C has centrifugal drift. Drift-velocity increases as the eye moves away from the null position, so that the position of the eyes increases exponentially with time. Such instability is commonly observed in humans with congenital nystagmus. It has also been observed in cases of cerebellar pathology (Zee, Leigh, & Mathieu-Millaire, 1980) and can be induced by one hour of adaptation with visual-vestibular conflict (Tiliket et al., 1994).

For some of the plots in Figs. 3 and 6, the linear model of (3) is a reasonable approximation, so that the basic classification of integrators as unbalanced (biased), leaky, or unstable is applicable. For example, all of the fish in Fig. 3, except for fish F, showed unidirectional drift in the light, indicating an integrator with imbalance in the nasal direction. At the end of the dark period in Fig. 6, the velocity–position relationships were all fairly linear, had negative slope, and except for the fourth fish, intersected the horizontal axis. These integrators are properly classified as leaky.

Some of the plots in Fig. 3 that show a marked downward concavity and non-monotonic behavior suggest that a linear  $P$ – $V$  plot may only be an approximation to the actual behavior. For the right eyes of fish B and C in the dark, the  $P$ – $V$  relationship intersects the horizontal axis at two points, which means that there are two null positions at which drift-velocity vanishes, on average. At the nasal null position, the slope is positive, indicating that the integrator is unstable about this point. At the temporal null position, the slope is negative, indicating that the integrator is leaky. This type of behavior is clearly qualitatively different from any of the behaviors in the classic terminology based on linear models (i.e., Eq. (3)) and suggests that in some cases the  $P$ – $V$  relationship must be generalized to

$$\frac{dE}{dt} = f(E) \quad (4)$$

where  $f(E)$  is a non-linear function. Another apparently non-linear behavior observed in many fish is an increased nasal drift at temporal eye positions. This is most clear in the light behaviors Fig. 3, where the velocity–position relationships for fish A, B, C, E, and G are flat over most of the position range, but the slope becomes more negative at the temporal extreme. Such a change in slope cannot be captured by the linear model of (3).

Non-linear position–velocity relationships, as in (4), cannot be explained by distributed feedback models that

have only one integrating mode (Kamath & Keller, 1976). More recent models that incorporate multiple modes (Cannon et al., 1983), recruitment thresholds and saturation (Seung, Lee, Reis, & Tank, 2000), or cellular bistability (Goldman et al., 2002; Koulakov, Raghavachari, Kepecs, & Lisman, 2002) could explain the relationship observed.

#### 4.4. Saccades, vergence, and stretch movements

The back-and-forth pattern of saccades and the horizontal range of motion (30°) observed in the present study was similar to that reported in previous goldfish studies (Easter, 1971, 1975; Hermann et al., 1971; Johnstone et al., 1969; Pastor et al., 1991). Hermann et al. (1971) compared freely swimming to spinalized goldfish and found similarities between the two conditions with respect to saccade patterns and ranges of motion. With respect to saccades in the spinalized subjects, they reported asynchrony, in that one eye typically led the other by 20–60 ms. The other previous studies reported synchrony to a precision of 10–20 ms. Using a larger group of subjects, a more sensitive measurement system, and more powerful data-analytic methods, we observed that in the majority of saccades, the two eyes reach half-maximum velocity within 5 ms of each other.

The time course of eye velocity during a saccade that we observed (rapid acceleration, plateauless peak, less rapid deceleration) was similar to that previously reported in goldfish (Easter, 1975) and humans. The current study is also in agreement with data from Easter (1975) regarding the relationship between saccade amplitude and maximum velocity (linear up to 20° with a slope of about 20 deg/s/deg). In humans, the slope is about 30 deg/s/deg and the curve is sublinear above 15°–20° (Collewijn, Erkelins, & Steinman, 1988). We also observed this sublinearity, but the sublinear region was small because few goldfish saccades are larger than 25°.

In foveated, frontal-eyed animals such as humans, the directions of gaze of the left and right eyes are tightly correlated so that objects of interest will be cast onto both foveas simultaneously. Goldfish are lateral-eyed: each eye has a 190° field of view (Charman & Tucker, 1973; Trevarthen, 1968), with only 60° of overlap frontally between the two eyes (Hester, 1968). Goldfish are also afoveate: photoreceptor density in the goldfish retina varies with location by only 2–4-fold (Hester, 1968), compared to 10–20-fold in humans (Curcio, Sloan, Kalina, & Hendrickson, 1990). Nonetheless, we observed significant correlation between the two eye positions, in agreement with all previous studies of goldfish.

Every 2–3 min, both eyes simultaneously undergo a large temporal, ventral excursion. These motions have been previously referred to as “stretches” or “blinks”. Their function is unknown. Easter (1971) observed that

the positions of the eyes during the first fixation after a stretch were typically bi-temporal, or highly divergent. Pastor et al. (1991) showed data from one goldfish in which the first post-stretch fixation was in the center of the range of motion for each eye. They suggested that stretches may play a role in recentering the eyes. In the present study, 83% of goldfish consistently exhibited highly divergent, temporal post-stretch positions; the other 17% consistently exhibited centered post-stretch positions.

We have not found any previous reports of the 5°–15° dorsal shift in vertical eye position which occurs when the lights are turned off. This was observed in all subjects. We do not speculate here about its cause or functional significance.

#### 4.5. Behavioral significance of steady fixation: maintenance of visual acuity

In order to avoid image blurring due to retinal slip, the eyes must be held stationary relative to the image that they are collecting. In humans, it has been shown that visual acuity is degraded if the retinal-slip velocity exceeds 2–3 deg/s (Barnes & Smith, 1981; Murphy, 1978; Westheimer & McKee, 1975). Human eye drift-velocities in the dark are typically less than 1.5 deg/s (Becker et al., 1973; Hess et al., 1985). These authors observed centripetal drifts (temporal drift in nasal positions, nasal drift in temporal positions) throughout the horizontal range of motion of the eye. Drift-velocity increased approximately linearly with increasingly eccentric positions. In complete darkness, vision is not possible, so the stationarity of the eyes is immaterial. But the good fixation-holding performance in the dark suggests that the oculomotor integrator is capable of holding the eyes still enough to avoid visual acuity degradation even without using visual feedback signals.

Because human visual acuity (about 1 min of arc (Wertheim, 1887)) is at least 20 times sharper than that of the goldfish (20 min to one degree, Hester, 1968; Hodos & Yolen, 1976; Northmore & Dvorak, 1979), it is likely that the goldfish visual system is more tolerant of eye drifts than the human visual system. Nonetheless, the drift-velocities we observed in the goldfish were of similar magnitude (less than 1.5 deg/s) to that reported in humans. Thus, the fixation stability of the goldfish oculomotor integrator is adequate to avoid visual-acuity-degrading levels of retinal slip.

#### Acknowledgements

The authors would like to thank Mark Goldman and Guy Major for their very helpful critical review of the manuscript. Support was provided, in part, by NIH/NIMH R01 MH068030-01 to DW Tank and grants

from the Packard foundation and Howard Hughes Medical Institute to HS Seung.

#### References

- Aksay, E., Baker, R., Seung, H. S., & Tank, D. W. (2000). Anatomy and discharge properties of pre-motor neurons in the goldfish medulla that have eye-position signals during fixations. *Journal of Neurophysiology*, *84*, 1035–1049.
- Arnold, D. B., & Robinson, D. A. (1991). A learning network model of the neural integrator of the oculomotor system. *Biological Cybernetics*, *64*, 447–454.
- Arnold, D. B., & Robinson, D. A. (1992). A neural network model of the vestibulo-ocular reflex using a local synaptic learning rule. *Philosophical Transactions of the Royal Society of London, Series B*, *337*, 327–330.
- Barnes, & Smith (1981). The effects of visual discrimination of image movements across the retina. *Aviation Space and Environmental Medicine*, *52*(8), 466–472.
- Becker, W., & Klein, H.-M. (1973). Accuracy of saccadic eye movements and maintenance of eccentric eye positions in the dark. *Vision Research*, *13*, 1021–1034.
- Cannon, S. C., & Robinson, D. A. (1987). Loss of the neural integrator of the oculomotor system from brain stem lesions in monkey. *Journal of Neurophysiology*, *57*, 1383–1409.
- Cannon, S. C., Robinson, D. A., & Shamma, S. (1983). A proposed neural network for the integrator of the oculomotor system. *Biological Cybernetics*, *49*, 127–136.
- Charman, W. N., & Tucker, J. (1973). The optical system of the goldfish eye. *Vision Research*, *13*(1), 1–8.
- Collewijn, G., Erkelens, C. J., & Steinman, R. M. (1988). Binocular coordination of human horizontal saccadic eye movements. *Journal of Physiology (London)*, *484*, 157–182.
- Corbett, J. J., Jacobson, D. M., Thompson, H. S., Hart, M. N., & Albert, D. W. (1989). Downbeating nystagmus and other ocular motor defects caused by lithium toxicity. *Neurology*, *39*(4), 481–487.
- Curcio, C. A., Sloan, K. R., Kalina, R. E., & Hendrickson, A. E. (1990). Human photoreceptor topography. *Journal of Comparative Neurology*, *292*(4), 497–523.
- Easter, S. S. (1971). Spontaneous eye movements in the goldfish. *Vision Research*, *11*, 333–342.
- Easter, S. S. (1975). The time course of saccadic eye movements in goldfish. *Vision Research*, *15*, 405–409.
- Goldman, M. S., Kaneko, C. R., Major, G., Aksay, E., Tank, D. W., & Seung, H. S. (2002). Linear regression of eye velocity on eye position and head velocity suggests a common oculomotor neural integrator. *Journal of Neurophysiology*, *88*(2), 659–665.
- Graf, W., Spencer, R., Baker, H., & Baker, R. (1997). Excitatory and inhibitory pathways to the extraocular motor nuclei in goldfish. *Journal of Neurophysiology*, *77*, 2765–2779.
- Hermann, H. T., & Constantine, M. M. (1971). Eye movements in the goldfish. *Vision Research*, *11*, 313–331.
- Hess, K., Reisine, H., & Dursteler, M. (1985). Normal eye drift and saccadic drift correction in darkness. *Neuro-ophthalmology*, *5*(4), 247–252.
- Hester, F. J. (1968). Visual contrast thresholds of the goldfish (*Carassius auratus*). *Vision Research*, *8*, 1315–1335.
- Hodos, W., & Yolen, N. M. (1976). Behavioral correlates of “tectal compression” in goldfish. II. Visual acuity. *Brain Behavior and Evolution*, *13*(6), 468–474.
- Johnstone, F. R., & Mark, R. F. (1969). Evidence for efference copy for eye movements in fish. *Comparative Biochemistry and Physiology*, *30*, 931–939.
- Jones, G. M. (1977). Plasticity in the adult vestibulo-ocular reflex arc. *Philosophical Transactions of the Royal Society of London Series B—Biological Sciences*, *278*(961), 319–334.

- Kamath, B. Y., & Keller, E. L. (1976). A neurological integrator for the oculomotor control system. *Mathematical Biosciences*, 30, 341–352.
- Kompf, D., & Piper, H. F. (1987). Eye movements and vestibulo-ocular reflex in the blind. *Journal of Neurology*, 234(5), 337–341.
- Koulakov, A. A., Raghavachari, S., Kepecs, A., & Lisman, J. E. (2002). Model for a robust neural integrator. *Nature Neuroscience*, 5(8), 775–782.
- Leech, J., Gresty, M., Hess, K., & Rudge, P. (1977). Gaze failure, drifting eye movements and centripetal nystagmus in cerebellar disease. *British Journal of Ophthalmology*, 61, 774–781.
- Leigh, R. J., & Zee, D. S. (1980). Eye movements of the blind. *Vision Research*, 19, 328–331.
- Leigh, R. J., & Zee, D. S. (1991). *The neurology of eye movements*. Philadelphia: Davis.
- Murphy, B. J. (1978). Pattern thresholds for moving and stationary gratings during smooth eye movement. *Vision Research*, 18(5), 521–530.
- Neumeyer, C. (1984). On spectral sensitivity in the goldfish. Evidence for neural interactions between different “cone mechanisms”. *Vision Research*, 24(10), 1223–1231.
- Northmore, D. P., & Dvorak, C. A. (1979). Contrast sensitivity and acuity of the goldfish. *Vision Research*, 19(3), 255–261.
- Pastor, A. M., Cruz, R. R. d. L., & Baker, R. (1994). Eye position and eye velocity integrators reside in separate brainstem nuclei. *Proceedings of the National Academy of Sciences of the United States of America*, 91, 807–811.
- Pastor, A. M., Torres, B., Delgado-Garcia, J. M., & Baker, R. (1991). Discharge characteristics of medial rectus and abducens motoneurons in the goldfish. *Journal of Neurophysiology*, 66, 2125–2140.
- Robinson, D. A. (1963). A method of measuring eye movement using a scleral search coil in a magnetic field. *IEEE Transactions on Bio-Medical Electronics* (October), 137–145.
- Rottach, K. G., Wohlgemuth, W. A., Dzaja, A. E., Eggert, T., & Straube, A. (2002). Effects of intravenous opioids on eye movements in humans possible mechanisms. *Journal of Neurology*, 249(9), 1200–1205.
- Seung, H. S. (1996). How the brain keeps the eyes still. *Proceedings of the National Academy of Sciences of the United States of America*, 93, 13339–13344.
- Seung, H. S., Lee, D. D., Reis, B. Y., & Tank, D. W. (2000). Stability of the memory of eye position in a recurrent network of conductance-based model neurons. *Neuron*, 26, 259–271.
- Skavenski, A. A., & Steinman, R. M. (1970). Control of eye position in the dark. *Vision Research*, 10, 193–203.
- Tiliket, C., Shelhamer, M., Roberts, D., & Zee, D. S. (1994). Short-term vestibulo-ocular reflex adaptation in humans. I. Effect on the ocular velocity-to-position neural integrator. *Experimental Brain Research*, 100, 316–327.
- Trevarthen, C. (1968). Vision in fish: the origins of the visual frame for action in vertebrates. In D. Ingle (Ed.), *The central nervous system and fish behavior* (pp. 61–94). University of Chicago Press.
- Wertheim, T. (1887). Über die Zahl der Sehnheit im mittleren Theile der Netzhaut. *von Graefes Archiv für klinische und experimentelle Ophthalmologie*, 33(2), 137–146.
- Westheimer, G., & McKee, S. P. (1975). Visual acuity in the presence of retinal-image motion. *Journal of the Optical Society of America*, 65(7), 847–850.
- Zee, D. S., Leigh, R. J., & Mathieu-Millaire, F. (1980). Cerebellar control of ocular gaze stability. *Annals of Neurology*, 7, 37–40.